Orientational pinning and transverse voltage: Simulations and experiments in square Josephson junction arrays

V. I. Marconi, S. Candia, P. Balenzuela,* H. Pastoriza, and D. Domínguez
Centro Atómico Bariloche, 8400 San Carlos de Bariloche, Rio Negro, Argentina

P. Martinoli
Institut de Physique, Université de Neuchâtel, CH-2000 Neuchâtel, Switzerland
(Received 14 January 2000)

We study the dependence of the transport properties of square Josephson Junction arrays with the direction of the applied dc current, both experimentally and numerically. We present computational simulations of current–voltage curves at finite temperatures for a single vortex in an array of $L\times L$ junctions ($Ha^2/\Phi_0=f=1/L^2$), and experimental measurements in 100×1000 arrays under a low magnetic field corresponding to $f\approx0.02$. We find that the transverse voltage vanishes only in the directions of maximum symmetry of the square lattice: the [10] and [01] direction (parallel bias) and the [11] direction (diagonal bias). For orientations different from the symmetry directions, we find a finite transverse voltage that depends strongly on the angle ϕ of the current. We find that vortex motion is pinned in the [10] direction ($\phi=0$), meaning that the voltage response is insensitive to small changes in the orientation of the current near $\phi=0$. We call this phenomenon orientational pinning. This leads to a finite transverse critical current for a bias at $\phi=0$ and to a transverse voltage for a bias at $\phi\neq0$. On the other hand, for diagonal bias in the [11] direction the behavior is highly unstable against small variations of ϕ, leading to a rapid change from zero transverse voltage to a large transverse voltage within a few degrees. This last behavior is in good agreement with our measurements in arrays with a quasidiagonal current drive.

I. INTRODUCTION

The interaction between the periodicity of vortex lattices (VL's) and periodic pinning potentials in superconductors has raised a great interest both in equilibrium systems[1–9] and in driven nonequilibrium systems.[10–13] Several techniques have been used to artificially fabricate periodic pinning in superconducting samples: thickness modulated films,[1] wire networks,[2] Josephson junction arrays,[3,4] magnetic dot arrays,[5] submicron hole lattices,[6] and pinning induced by Bitter decoration.[7]

The ground states of these systems, which result from the competition between the vortex–vortex and the vortex–pinning interactions, can be either commensurate or incommensurate vortex structures depending on the vortex density.[1,9,14] These commensurability effects in the ground state vortex configurations lead to enhanced critical currents and resistance minima for the ''matching'' and for the ''fractional'' (submatching) vortex densities where the VL is strongly pinned. At finite temperatures, it has been shown numerically that there are both a depinning and a melting transition, which can occur either sequentially or simultaneously depending on the magnetic field.[8]

Very recently, the physics of driven vortices under periodic pinning has been studied numerically both at zero temperature[10,11] and at finite temperatures.[12,13] At $T=0$ there is a complex variety of dynamic phases.[10] At finite T there are two dynamic transitions when increasing temperature at high drives: there is first a transverse depinning and second a melting transition of the moving vortex lattice.[12]

Most of the effects of periodic pinning that have been studied are related to commensurability phenomena and the breaking of translational symmetry in these systems. Less studied is the effect of the breaking of rotational symmetry in periodic pinning potentials, in particular, regarding transport properties. One question of interest is how the motion of vortices changes when the direction of the driving current is varied. If there is rotational symmetry, the vortex motion and voltage response should be insensitive to the choice of the direction of the current. However, it is clear that in a periodic pinning potential the dynamics may depend on the direction of the current. For example, in square Josephson junction arrays (JJA's) it has been found experimentally that the existence of fractional giant Shapiro steps (FGGS's) depends on the orientation of the current bias. When the JJA is driven in the [11] direction the FGGS are absent, while they are very large when the drive is in the [10] direction.[15] Another example of more recent interest is the phenomenon of transverse critical current in superconductors with pinning.[16] It has been found numerically that for a VL driven with a high current there is a transverse critical current when an additional small bias is applied in the perpendicular direction.[10–12] Furthermore, when the transverse bias is increased it is possible to have a rich behavior with a Devil's staircase in the transverse voltage.[11] However, there has not been experimental measurements of the existence of transverse voltages and transverse pinning effects.

In this paper we will study in detail both numerically and experimentally the breaking of rotational invariance in square JJA. In this case, the discrete lattice of Josephson junctions induces a periodic egg-carton potential for the motion of vortices.[4] Here we will study how the voltage response depends on the angle of the current with respect to the lattice directions of the square JJA. We will show both numerically and experimentally that there are preferred directions for vortex motion for which there is orientational pinning. This leads to an anomalous transverse voltage when vortices are driven in directions different from the symmetry

directions. An analogous effect of a transverse voltage due to the guided motion of vortices has been observed experimentally in YBCO superconductors with twin boundaries.[17] Another related case is the intrinsic breaking of rotational symmetry of *d*-wave superconductivity, which causes an angle-dependent transverse voltage for large currents, which has been studied theoretically in Ref. 18. Here we will show the differences and similarities of the square JJA with these problems.

The paper is organized as follows. In Sec. II we present the model equations for the dynamics of the JJA, which will be solved in the numerical simulations. In Sec. III we describe the experimental details of the JJA used in the measurements. In Sec. IV we will present our results for both the simulations and for the experiments. In particular, we will present experiments corresponding to the orientation for which the effect of a transverse voltage is maximum. Finally in Sec. V we will compare our results with other similar effects and discuss future directions of study.

II. THEORETICAL MODEL

We study the dynamics of JJA using the resistively shunted junction (RSJ) model for the junctions of the square network.[19–22] In this case, the current flowing in the junction between two superconducting islands in a JJA is modeled as the sum of the Josephson supercurrent and the normal current:

$$I_\mu(\mathbf{n}) = I_0 \sin\theta_\mu(\mathbf{n}) + \frac{\Phi_0}{2\pi c R_N}\frac{\partial \theta_\mu(\mathbf{n})}{\partial t} + \eta_\mu(\mathbf{n},t), \quad (1)$$

where I_0 is the critical current of the junction between the sites $\mathbf{n}$ and $\mathbf{n}+\mu$ in a square lattice $[\mathbf{n}=(n_x,n_y), \mu=\hat{\mathbf{x}},\hat{\mathbf{y}}]$, R_N is the normal state resistance, and

$$\theta_\mu(\mathbf{n}) = \theta(\mathbf{n}+\mu) - \theta(\mathbf{n}) - A_\mu(\mathbf{n}) = \Delta_\mu\theta(\mathbf{n}) - A_\mu(\mathbf{n}) \quad (2)$$

is the gauge invariant phase difference with

$$A_\mu(\mathbf{n}) = \frac{2\pi}{\Phi_0}\int_{\mathbf{n}a}^{(\mathbf{n}+\mu)a} \mathbf{A}\cdot d\mathbf{l}. \quad (3)$$

The thermal noise fluctuations η_μ have correlations

$$\langle \eta_\mu(\mathbf{n},t)\,\eta_{\mu'}(\mathbf{n}',t')\rangle = \frac{2kT}{R_N}\delta_{\mu,\mu'}\delta_{\mathbf{n},\mathbf{n}'}\delta(t-t'). \quad (4)$$

In the presence of an external magnetic field H we have

$$\Delta_\mu \times A_\mu(\mathbf{n}) = A_x(\mathbf{n}) - A_x(\mathbf{n}+\mathbf{y}) + A_y(\mathbf{n}+\mathbf{x}) - A_y(\mathbf{n}) = 2\pi f, \quad (5)$$

where $f = Ha^2/\Phi_0$ and a is the array lattice spacing. We take periodic boundary conditions (p.b.c's) in both directions in the presence of an external current $\mathbf{I}=(I_x,I_y)$ in arrays with $L\times L$ junctions.[23] The vector potential is taken as

$$A_\mu(\mathbf{n},t) = A^0_\mu(\mathbf{n}) - \alpha_\mu(t), \quad (6)$$

where in the Landau gauge $A^0_x(\mathbf{n}) = -2\pi f n_y$, $A^0_y(\mathbf{n}) = 0$, and $\alpha_\mu(t)$ allows for total voltage fluctuations under periodic boundary conditions. In this gauge the p.b.c. for the phases are[12,23]

$$\theta(n_x+L,n_y) = \theta(n_x,n_y), \quad (7)$$

$$\theta(n_x,n_y+L) = \theta(n_x,n_y) - 2\pi f L n_x.$$

The condition of a total current flowing in the x and y directions

$$I_x = \frac{1}{L^2}\left[\sum_{\mathbf{n}} I_0 \sin\theta_x(\mathbf{n}) + \eta_x(\mathbf{n},t)\right] + \frac{\hbar}{2eR_N}\frac{d\alpha_x}{dt},$$

$$I_y = \frac{1}{L^2}\left[\sum_{\mathbf{n}} I_0 \sin\theta_y(\mathbf{n}) + \eta_y(\mathbf{n},t)\right] + \frac{\hbar}{2eR_N}\frac{d\alpha_y}{dt} \quad (8)$$

determines the dynamics of $\alpha_\mu(t)$.[23] We also consider local conservation of current

$$\Delta_\mu \cdot I_\mu(\mathbf{n}) = \sum_\mu I_\mu(\mathbf{n}) - I_\mu(\mathbf{n}-\mu) = 0. \quad (9)$$

After Eqs. (1), (8), and (9) we obtain the following set of dynamical equations for the phases;[12,23]

$$\Delta^2_\mu \frac{\partial\theta(\mathbf{n})}{\partial t} = -\Delta_\mu\cdot[S_\mu(\mathbf{n}) + \eta_\mu(\mathbf{n},t)], \quad (10)$$

$$\frac{\partial\alpha_\mu}{\partial t} = I_\mu - \frac{1}{L^2}\sum_{\mathbf{n}}[S_\mu(\mathbf{n}) + \eta_\mu(\mathbf{n},t)], \quad (11)$$

where

$$S_\mu(\mathbf{n}) = \sin[\Delta_\mu\theta(\mathbf{n}) - A^0_\mu(\mathbf{n}) - \alpha_\mu], \quad (12)$$

we have normalized currents by I_0, time by $\tau_J = 2\pi c R_N I_0/\Phi_0$, temperature by $I_0\Phi_0/2\pi k_B$, and the discrete Laplacian is

$$\Delta^2_\mu\theta(\mathbf{n}) = \theta(\mathbf{n}+\hat{\mathbf{x}}) + \theta(\mathbf{n}-\hat{\mathbf{x}}) + \theta(\mathbf{n}+\hat{\mathbf{y}}) + \theta(\mathbf{n}-\hat{\mathbf{y}}) - 4\theta(\mathbf{n}). \quad (13)$$

The Langevin dynamical equations (10)–(11) are solved with a second order Runge–Kutta–Helfand–Greenside algorithm with time step $\Delta t = 0.1\tau_J$ and integration time $5000\tau_J$ after a transient of $2000\tau_J$. The discrete Laplacian is inverted with a fast Fourier+tridiagonalization algorithm as in Ref. 22. We calculate the time average of the total voltage as

$$V_x = \langle v_x(t)\rangle = \langle d\alpha_x(t)/dt\rangle,$$

$$V_y = \langle v_y(t)\rangle = \langle d\alpha_y(t)/dt\rangle, \quad (14)$$

with voltages normalized by $R_N I_0$.

We study the JJA under a magnetic field corresponding to a single vortex in the array, $f = 1/L^2$, and system sizes of $L\times L$ junctions, with $L = 32,64$. We apply a current I at an angle ϕ with respect to the [10] lattice direction

$$I_x = I\cos\phi,$$

$$I_y = I\sin\phi. \quad (15)$$

We define the longitudinal voltage as the voltage in the direction of the applied current

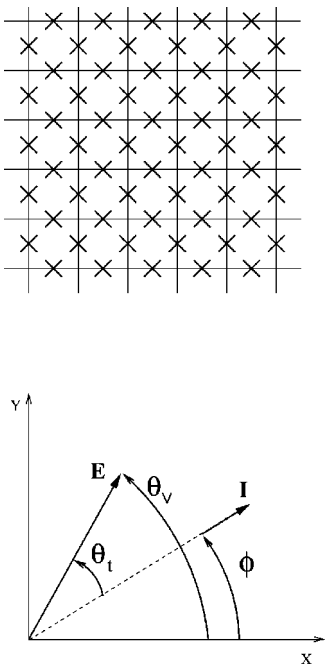

FIG. 1. (Top) Schematic representation of a square Josephson junction array, the crosses indicate Josephson junctions. (Bottom) Definition of angles with respect to the x and y axis of the array. The vector of applied current $\mathbf{I}=(I_x,I_y)$ forms an angle ϕ respect to the x axis. The vector of electric field $\mathbf{E}=(V_x,V_y)$ forms an angle θ_v with respect to the x-axis and an angle θ_t with respect to the current $\mathbf{I}$.

$$V_l = V_x \cos\phi + V_y \sin\phi, \tag{16}$$

and the transverse voltage

$$V_t = -V_x \sin\phi + V_y \cos\phi. \tag{17}$$

From the voltage response, we define the transverse angle as

$$\tan\theta_t = V_t / V_l \tag{18}$$

and the voltage angle as

$$\tan\theta_v = V_y / V_x, \tag{19}$$

i.e., $\theta_t = \theta_v - \phi$, (see Fig. 1). When the vortices move in the direction perpendicular to the current, there is no transverse voltage, therefore $\theta_t = 0$ and $\theta_v = \phi$.

III. EXPERIMENTAL SETUP

We measured current–voltage (I–V) characteristics of square proximity–effect Pb/Cu/Pb Josephson arrays with the current applied in different directions.

The samples consist of 2500-Å-thick cross-shaped Pb islands on top of a continuous 2500-Å-thick copper film. Copper, and subsequently lead, were thermally evaporated onto a silicon substrate within the same evaporator. An array of 1000×1000 lead islands were defined by photolithographic patterning followed by an Ar ion etching. The cell parameter of the resulting array was 10 μm with junctions 2-μm wide and a separation of 1μm. A second photolithography step was used to define a 1×10 mm^2 strip with current and voltage (longitudinal and transversal) contacts. This mask was manually aligned in the [10] and [11] directions for different samples.

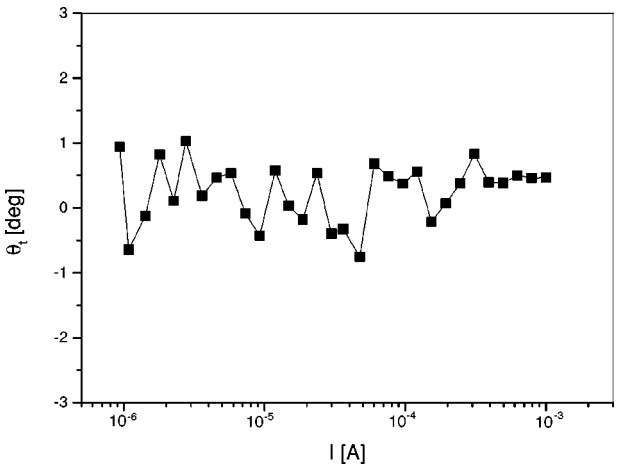

FIG. 2. Experimental voltage angle as a function of the applied current for a square JJA, with $f=1/25$ and $\tau=0.12$. The current was applied in the [10] direction (parallel bias).

The six-terminal measurements were made using a programable dc current source and a two channel nanovoltmeter (HP 34420A), with each channel measuring the longitudinal and transversal voltage, respectively. The arrays were coooled up to 1.25 K in a pumped ^{4}He cryostat shielded by μ-metal. A superconducting solenoid was used to null the remaining ambient magnetic field ($\approx$15 mG), and apply fields to the sample. The typical periodic-in-field response in the resistance was observed extending in a large number of periods, which was used to determine the frustration applied to the sample.

IV. RESULTS

A. Breaking of rotational invariance: model predictions

The square lattice has two directions of maximum symmetry: the [10] and the [11] directions (and the ones obtained from them by $\pi/2$ rotations), which correspond to the directions of reflection symmetry. When the current bias is in the [10] direction, the angle of the current is $\phi=0$, and we call it a ''parallel'' bias. When the current bias is in the [11] direction, the angle of the current is $\phi=\pi/4=45°$, and we call it a ''diagonal'' bias.

In the case of the parallel bias we find both experimentally and numerically that the transverse voltage is zero (in agreement with the reflection symmetry). This corresponds to vortex motion in the direction perpendicular to the current ($\theta_t=0$). Shown in Fig. 2 are the experimental results of θ_t as a function of the applied current, for a JJA with the current fed in the [10] direction. This measurement was taken for a frustration of $f=0.02$, and for a reduced temperature $\tau=0.12$, although similar results were obtained for different frustrations and temperatures.

In the I–V curve for the longitudinal voltage we find numerically a critical current corresponding to the single vortex depinning $I_c^{[10]}=0.1$,[4] as shown in Fig. 3(a). Above I_c it is possible to distinguish three regimes in the numerical results:[20,21] (**A**) a single vortex regime for $0.1<I<0.85$, where the I–V is quasilinear and dissipation is caused by

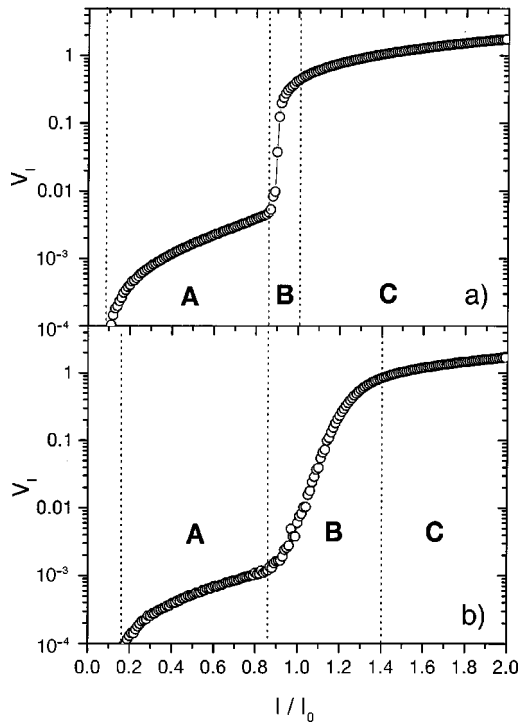

FIG. 3. Current–voltage characteristics at $T=0$ for Josephson junction arrays with $f=1/L^2$ and $L=64$ obtained from simulations: (a) for the parallel bias case $\phi=0$; (b) for the diagonal bias case $\phi=\pi/4$. Currents are normalized by I_0 and voltages by $R_N I_0$

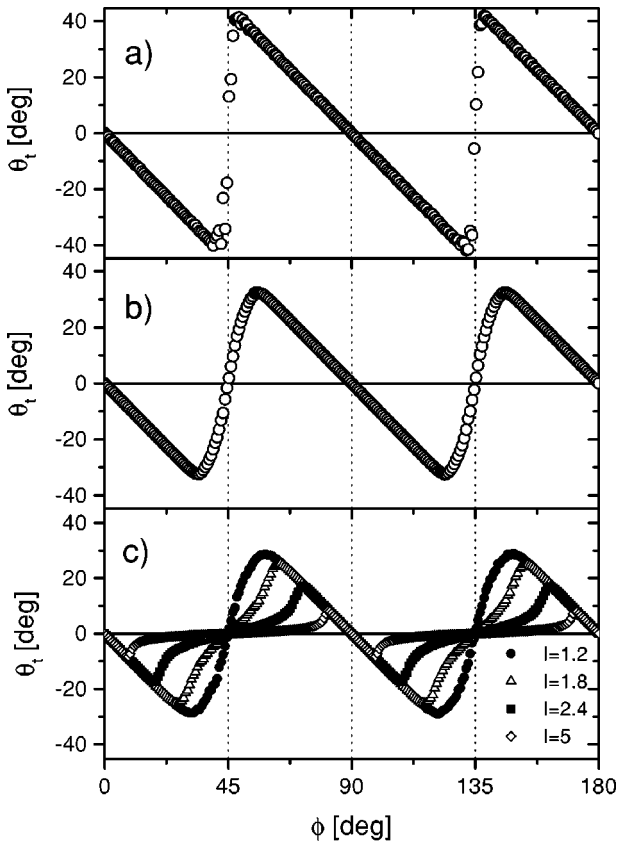

FIG. 4. Simulation results of the behavior of the transverse angle $\theta_t=\arctan(V_t/V_l)$ vs the angle of the current ϕ: (a) $T=0.01$ and $I=0.6$; (b) $T=0.01$ and $I=1.2$;(c) $T=0.05$ and different currents.

vortex motion; (**B**) an intermediate crossover regime for $0.85<I<1.0$; and (**C**) a resistive regime for $I>1.0$, where dissipation is caused by the ohmic shunt resistance and the I–V curve is linear. The vortex regime **A** can be described by the dynamics of a single collective degree of freedom: an overdamped particle moving in the periodic egg-carton potential,[4,20] although with a nonlinear viscosity.[21] The resistive regime **C** is also very simple; it can be represented by the behavior of a single junction at large currents, $\theta_\mu(\mathbf{n},t) \approx (2eR_N/\hbar)I_\mu t+\delta_\mu(\mathbf{n},t)$. The crossover regime **B** is characterized by a complex collective dynamics with an interplay of the vortex degree of freedom with spin waves excitations, and at finite temperatures there is also a steep increase of vortex–antivortex excitations in this regime.

In the case of the perfect diagonal bias, which is only attainable in the numerical model, we obtain similar results as in the parallel bias case. The transverse voltage is zero and therefore the vortex moves perpendicular to the current ($\theta_t=0$). In agreement with the prediction of Halsey,[14] the numerical I–V curve for V_l has a critical current of $I_c^{[11]}=\sqrt{2}I_c^{[10]}=0.1414$. The onset of the resistive regime **C** is also multiplied by a factor of $\sqrt{2}$, while the crossover regime **B** starts at nearly the same current as in the parallel bias case, see Fig. 3(b).

For orientations different than the symmetry directions, we always find both numerically and experimentally a finite transverse voltage. In order to see this, we show our numerical study of the voltage response when varying the orientation ϕ of the drive while keeping fixed the amplitude I of the current. In Fig. 4(a) we plot the transverse angle $\theta_t=\arctan(V_t/V_l)$ as a function of the angle of the current ϕ. We find that θ_t vanishes only in the maximum symmetry directions corresponding to angles $\phi=0,\pm 45°,\pm 90°,\ldots$, as discussed before. Furthermore, we see that for orientations near $\phi=0$, the transverse angle basically follows the current angle: $\theta_t\approx-\phi$. This is an indication that vortex motion is pinned in the lattice direction [10], since $V_y\approx 0$, meaning that the voltage angle is $\theta_v\approx 0$. Whenever the voltage response is insensitive to small changes in the orientation of the current, we will call this phenomenon *orientational pinning*. On the other hand, near $\phi=45°$ the transverse angle changes rapidly. We show in Figs. 4(b) and 4(c) the behavior of θ_t for different currents and temperatures. The θ_t vs ϕ curves become smoother around $\phi=45°$ for increasing current as well as for increasing T. At the same time, the magnitude of the transverse angle decreases when increasing the current for $I\gg 1$, or when increasing T.

A more direct evidence of the breaking of rotational symmetry can be seen in the parametric curves of $V_y(\phi)$ vs $V_x(\phi)$. In Fig. 5 we plot the values obtained numerically for the voltages V_y and V_x when varying the orientational angle ϕ for different values of the current amplitude I and the temperature. In the case of rotational symmetry we should have a perfect circle. In the set of plots of Fig. 5(a)–5(c), the current amplitude is fixed and the temperature is varied. In Fig. 5(a) we have $I=0.2$, near the onset of single vortex motion in the regime **A**. In this case most of the points are either on the axis $V_x=0$ or on the axis $V_y=0$, indicating strong orientational pinning in the lattice directions [10] or [01]. When increasing T the orientational pinning decreases

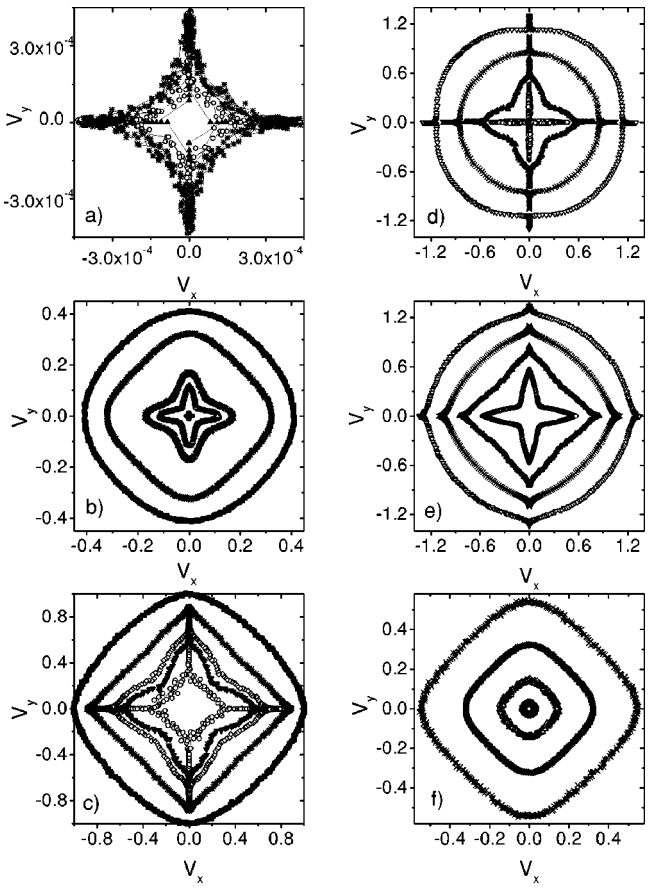

FIG. 5. Simulation results of the parametric curves $V_y(\phi)$ vs $V_x(\phi)$; (a) $I=0.2$, for (going outwards from the center) $T=0, T=0.01$, and $T=0.05$; (b) $I=0.6$ for $T=0.3, T=0.5, T=0.6, T=1.0$, and $T=1.4$; (c) $I=1.2$ for $T=0, T=0.05, T=0.1, T=0.3$, and $T=1.0$; (d) $T=0.05$ for (going outwards from the center) $I=1.0, I=1.2, I=1.4$, and $I=1.6$; (e) $T=0.2$ for $I=1.0, I=1.2, I=1.4$, and $I=1.6$; (f) $T=1.0$ for $I=0.2, I=0.4, I=0.6$, and $I=0.8$.

and the length of the ''horns'' in the x and y axis decreases. Figure 5(b) corresponds to $I=0.6$, near the end of regime **A** when the vortex is moving fast. In this case the horns have disappeared and orientational pinning is lost. However, the breaking of rotational symmetry is still present in the star-shaped curves that we find at low T. The dip at 45° in the stars is because in this direction the voltages are minimum, since the critical current is maximum in this case, $I_c^{[11]}=0.1\sqrt{2}$. When increasing the temperature, the stars tend to the circular shape of rotational invariance. The parametric curves in the crossover regime **B** also have star shaped behavior at low T which tends to circles when increasing T. Above the onset of the resistive regime **C** the ''horned'' curves reappear [Fig. 5(c)]. In this case the orientational pinning corresponds to the locking of ohmic dissipation in the junctions in one of the lattice directions, either [10] or [01]. Once again, when increasing T the horned structure shrinks, and the curves evolve continuously from square to circular shapes.

The variation with current of the rotational parametric curves for a fixed temperature is shown in the numerical results of Figs. 5(d)–5(f). At a low temperature, $T=0.05$, we clearly see the horned structure of the curves for almost all the currents and even for large currents the circular curves

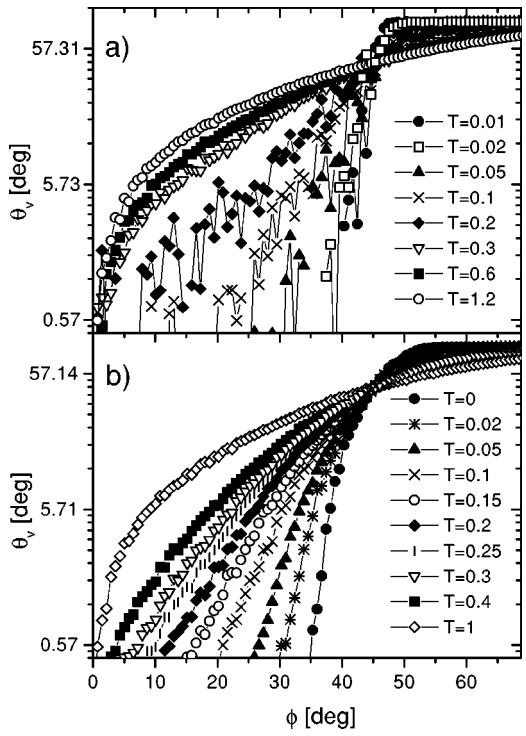

FIG. 6. Orientational pinning near $\phi=0$. Simulation results of voltage angle $\theta_v=\arctan(V_y/V_x)$ vs ϕ for different temperatures and (a) $I=0.6$; (b) $I=1.2$.

have horns [see Fig. 5(d)]. At an intermediate temperature, $T=0.2$, there are still some signatures of the orientational pinning [Fig. 5(e)], while for $T=1.2$ all the curves are smooth and rounded with a slightly square shape [Fig. 5(f)].

B. Orientational pinning near the [10] direction: Simulations and experiments

The orientational pinning characterizes the breaking of rotational symmetry in square arrays at low temperatures, as we have seen in the previous section. When the JJA is driven in any of the ''parallel'' directions, ϕ=0°,90°,180°, or 270° both vortex motion and dissipation are pinned along these directions. When the current is rotated a small angle, for example from the [10] direction, the dissipation remains pinned along the [10] direction ($V_x\neq 0$, $V_y=0$). This effect causes a finite transverse voltage, measured with respect to the direction of the current $V_t\approx -V_x\sin\phi$ and a transverse angle $\theta_t=-\phi$. The orientational pinning is lost at a given critical angle ϕ_c which depends on temperature and current. As we can see in Fig. 4(a), for very low T and for certain values of the current, the critical angle can reach values very close to 45°. This leads to a large transverse voltage in arrays driven near the [11] direction as we will discuss later in Sec. IV C.

Let us analyze now the behavior of the critical angle for orientational depinning ϕ_c . This can be studied numerically by looking at the angle of the voltage with respect to the [10] direction, $\theta_v=\arctan(V_y/V_x)$. For $\phi<\phi_c$ we have orientational pinning and therefore $\theta_v=0$, while for $\phi>\phi_c$ we have $\theta_v\neq 0$. Therefore, the onset of a finite θ_v defines the critical angle ϕ_c . In Fig. 6 we plot the numerically obtained θ_v as a function of ϕ for different currents and temperatures. There

are two cases of interest: for a current in the single vortex regime **A** [Fig. 6(a)] and for a current in the resistive regime **C** [Fig. 6(b)]. We find that in both cases there is clearly a finite ϕ_c which decreases with temperature. In the case of the single vortex regime **A**, we see that ϕ_c tends to vanish at a crossover temperature corresponding to the energy scale for vortex depinning,[4] $T_{\rm pin}\sim\Delta E_{\rm pin}\approx 0.2$. The notion of ''transverse critical current'' $I_{c,\rm tr}$ has been introduced recently in the theoretical work by Giamarchi and Le Doussal for driven vortex lattices in random pinning.[16] When a vortex structure is moving fast, it can still be pinned in the transverse direction. After applying a current in the direction perpendicular to the drive, a finite transverse critical current may exist at $T=0$. In the case of periodic pinning, a finite $I_{c,\rm tr}$ was also proposed due to conmensurability effects.[16] In particular, in the periodic egg-carton pinning of Josephson junction arrays it was found numerically in Ref. 12 that $I_{c,\rm tr}$ is finite in a wide range of temperatures for a system driven in the [10] direction. Here we see that due to the orientational pinning, a transverse critical current is finite only when the JJA is driven either in the [10] or [01] directions. In any other case it will be zero. Moreover, the critical angle in regime **A** can be interpreted as corresponding to a transverse critical current $I_{c,\rm tr}=I\sin\phi_c$ for a vortex driven by a longitudinal current $I_l=I\cos\phi_c$.

In Fig. 6(b) we see that for a current in the resistive regime **C** there is also a critical angle for the onset of transverse ohmic dissipation. In this case ϕ_c tends to vanish at a higher temperature above the Kosterlitz–Thouless transition $T_{\rm KT}\approx 0.9$.

The other lattice symmetry direction of interest corresponds to the case of ''diagonal'' bias, i.e., the [11] directions of ϕ=45°,135°,225°, and 315°. In this case, we have shown previously that the transverse voltage also vanishes. In agreement with this, we see both in Fig. 6(a) and 6(b) that all the curves cross in the point $(\phi,\theta_v)=(45°,45°)$, which corresponds to $\theta_t=\theta_v-\phi=0$. However, there is no orientational pinning in the [11] direction. On the contrary, in this direction any small deviation in the orientation of the current can cause a fast increase of the transverse voltage. In order to show this effect, we study numerically the ''diagonal voltage angle,'' which is measured with respect to 45°: $\theta_v'=\arctan(V_y-V_x)/(V_y+V_x)=\theta_v-\pi/4$, as a function of the deviation from the [11] direction, $\Delta\phi=\phi-\pi/4$, (see Fig. 7). We find that, in contrast to the case of Fig. 6, a small deviation from the symmetry direction leads to a large change in the voltage angle for any current and temperature. This shows that the [11] direction is highly unstable against small changes in the orientation of the current, leading to an anomalously large transverse voltage.

C. Transverse voltage near the [11] direction: Simulations and experiments

In Fig. 8(a) we show our experimental voltage–current characteristics for an array of 100×1000 junctions at a low temperature $T=1.25$ K and at a low magnetic field. The current is applied nominally in the [11] direction, but a small misalignment is possible in the setup of electrical contacts, therefore $\phi=45°\pm 5°$. We see that for low currents there is a very large value of the transverse voltage V_t, which is nearly

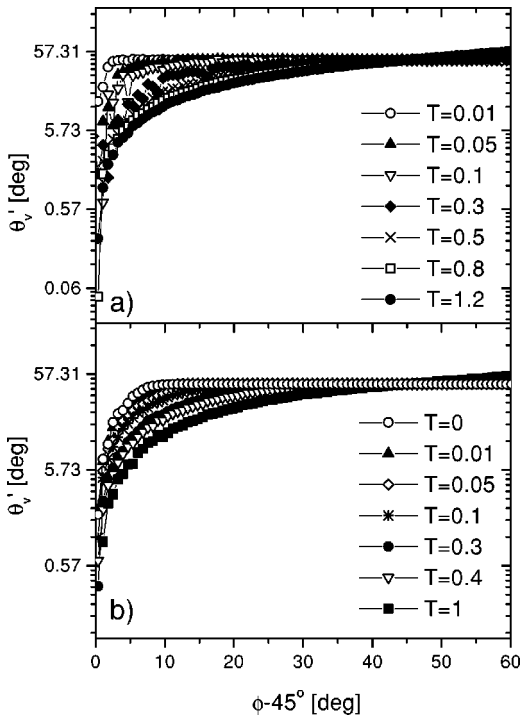

FIG. 7. Voltage angle with respect to the [11] direction $\theta_v'=\arctan(V_y-V_x)/(V_y+V_x)=\theta_v-\pi/4$ vs $\phi-\pi/4$ obtained numerically for different temperatures and (a) $I=0.6$; (b) $I=1.2$.

of the same magnitude as the longitudinal voltage V_l. The transverse voltage is maximum at a characteristic current I_m. Above I_m, V_t decreases with increasing current while V_l increases. It is remarkable that these results are very different from the I–V curve obtained numerically in Fig. 3, where $V_t=0$ at ϕ=45°. However, if we assume a misalignment of a few degrees with respect to the [11] direction we can reproduce the experimental results. In Fig. 8(b) we show the I–V curves obtained numerically for ϕ=40° and $T=0.02$. We see that for low currents V_t is close to V_l: $V_t\lesssim V_l$, similar to the experiment, and later V_t has a maximum at a current $I_m\approx 1/\cos\phi\approx 1.3$. This corresponds to the current for which the junctions in the x direction become critical ($I_x=1$). The range of currents we can measure experimentally is limited to regimes **B** and **C**, since we cannot fully access regime **A** of single vortex motion due to the small voltages involved in this case. Of course, in the simulations we can study the full range of currents, which is shown in Fig. 8(c). Here we see that near the vortex depinning current the transverse voltage is also very close to V_l in a small range of currents, then when increasing I they separate first inside regime **A**, and later in regime **B** the transverse voltage approaches the longitudinal voltage again.

As we saw in Fig. 4 the highest transverse voltage can be obtained for orientations near $\phi=45^o$. Therefore a slight misalignment of the array from the [11] direction is useful for studying the behavior of the transverse voltage both experimentally and numerically as a function of current and temperature.

In Fig. 9 we show the dependence of θ_t with current for different temperatures. The experimental results are shown in Fig. 9(a) where we find that θ_t first increases with current, it reaches a maximum value $\theta_t^{\rm max}(T)<45°$, and then for large

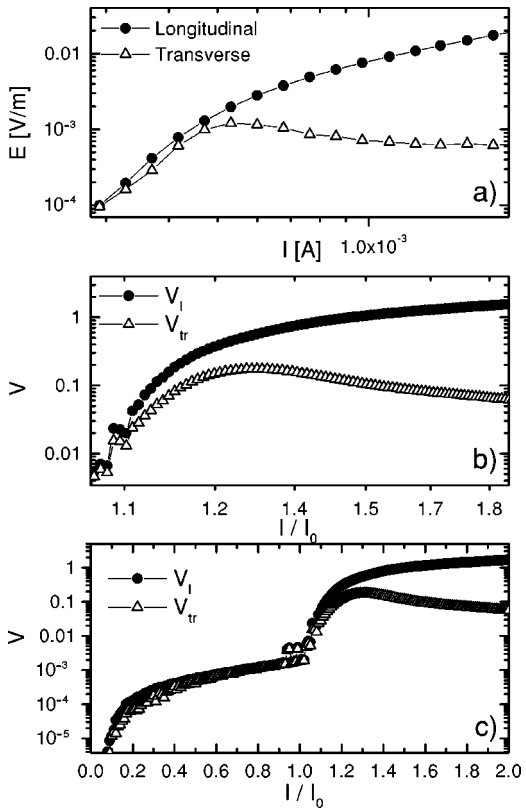

FIG. 8. (a) Experimental results of longitudinal and transverse voltage for a current near the [11] direction $\phi=45°\pm5$ at $T=1.25$K; (b) Longitudinal and transverse voltage obtained numerically for $\phi=40°$ at $T=0.02\,\hbar I_0/2ek_B$; (c) Idem (b) for an extended current range.

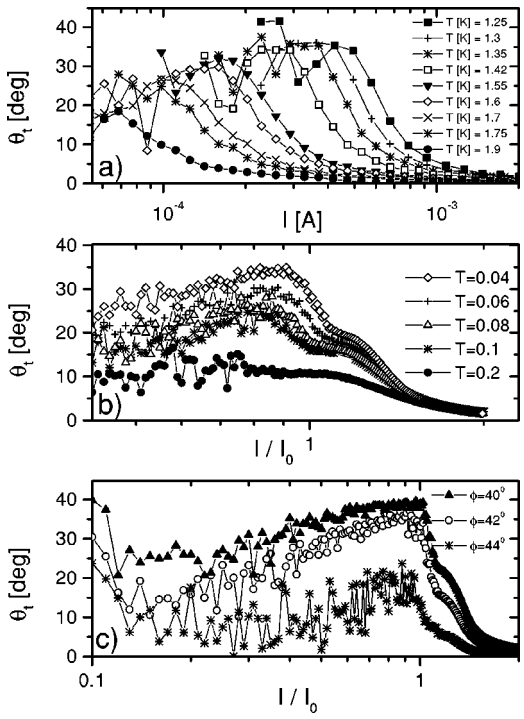

FIG. 9. (a) Experimental results of transverse angle θ_t vs current for $\phi=45°\pm5$ at different temperatures; (b) Numerical results of θ_t vs I for $\phi=40°$; (c) θ_t vs I at $T=0.02$ for different ϕ and full range of currents. Experimental temperatures are in Kelvin, simulation temperatures are in units of $\hbar I_0/2ek_B$.

currents θ_t tends to zero. In Fig. 9(b) we show that simulations with the RSJ model with $\phi=40°$ reproduce this behavior. Here we see that the maximum of the transverse angle is reached inside regime **B** well before the onset of the resistive regime. We also find that, when going deep into regime **C**, θ_t decreases with current: $\theta_t\to0$ for $I\gg I_m$. In Fig. 9(c) we show that a similar behavior is obtained for other values of ϕ close to 45°. We also observe here the full range of currents. We see that at the critical current the transverse angle θ_t first has a maximum, then it decreases rapidly in a small range of currents after which, for most of regime **A**, θ_t increases with I before reaching a second maximum value in the crossover regime **B**. This shows that there are two regimes where the effect of anomalous transverse voltage is maximum: near the vortex depinning current, due to orientational pinning of vortex motion; and near the Josephson junction critical current due to the orientational ''pinning'' of ohmic dissipation. Regretfully, we cannot measure the small voltages of the low current regime, therefore we were not able to observe experimentally the first maximum of θ_t.

In Fig. 10 we analyze the behavior of the transverse angle as a function of temperature. We plot the value of θ_t for a current near the maximum value of the transverse voltage at low T. We observe experimentally that θ_t decreases with temperature and in particular it has a sharp decrease at $T\approx1.5$ K, as we show in Fig. 10(a). On the other hand, in the simulation results we see a smooth decrease of θ_t with temperature [Fig. 10(b)]. The transverse angle becomes small at the depinning crossover temperature $T_{\rm pin}\approx0.2$. The fact that our experimental results show a sharper decrease with temperature than the simulations is possibly due to vortex collective effects. The simulation results presented here are focused in the motion of a single vortex in the periodic pinning of a square JJA. The vortex collective effects, which have to be studied for fields $f>1/L^2$, will be discussed elsewhere.[24]

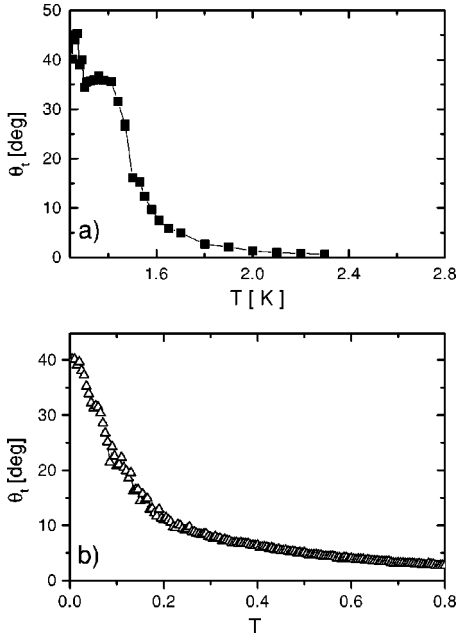

FIG. 10. (a) Experimental results of transverse angle vs T for $\phi=45°\pm5$ and $I=300\,\mu$A; (b) Numerical results of θ_t vs T for $\phi=40°$ and $I=0.85$.

V. DISCUSSION

In the egg-carton potential of a square JJA there are pinning barriers for vortex motion in all the directions. The direction with the lowest pinning barrier is the [10] direction. Therefore the strong orientational pinning we find here is in the direction of the lowest pinning for motion, i.e., the direction of easy flow for vortices. The presence of a strong orientational pinning leads to a large transverse voltage when the systems is driven away from the favorable direction, to the existence of a critical angle and to a transverse critical current. On the other hand, the [11] direction is the direction of the largest barrier for vortex motion in the egg-carton potential. In this case, the behavior is highly unstable against small variations in the angle of the drive, leading to a rapid change from zero transverse voltage to a large transverse voltage within a few degrees. Any misalignement of the current/voltage contacts as well as disorder in the junctions critical currents[24] can lead to a large transverse voltage for arrays with a diagonal bias. This explains the transverse voltage observed in our experimental measurements in JJA driven near the diagonal [11] orientation.

An analogous effect of orientational pinning has also been seen in experiments on YBCO superconductors with twin boundaries.[17] In this case, due to the correlated nature of the disorder, the direction for easy flow is the direction of the twins. A similar effect of horns in the parametric voltage curves are therefore observed in the direction corresponding to the twins. Also transport measurements show a large transverse voltage when the sample is driven at an angle with respect to the twin.

It is interesting to compare it with the angle-dependent transverse voltage calculated for *d*-wave superconductors.[18] Also in this case, the transverse voltage vanishes only in the [10] and [11] directions. However the θ_t vs ϕ curves are smooth in this case, since $\tan\theta_t \propto \sin 4\phi$.[18] This is because there is no pinning and the transverse voltage is caused only by the intrinsic nature of the *d*-wave ground state. On the other hand, the breaking of rotational symmetry studied here is induced by the pinning potential, and it results in nonsmooth responses like ''horned'' parametric voltage curves, critical angles, transverse critical currents, etc.

In superconductors with a square array of pinning centers, typically the pins are of circular shape and the size of the pins is much smaller than the distance between pinning sites.[9–11] In this case, the pinning barriers that vortices find for motion are the same in many directions. Therefore it is possible to have orientational pinning in many of the square lattice symmetry directions. This explains the rich structure of a Devil's staircase observed recently in the simulations of Reichhardt and Nori, where each plateau corresponds to orientational pinning in each of the several possible directions for orientational pinning. This interesting behavior is not possible in JJA, however, since the egg-carton pinning potential corresponds to the situation of square-shaped pinning centers with the pin size equal to the interpin distance. In this case the only possible directions for orientational pinning are the [10] and [01], as we have seen here.

It is worth noting that many experiments in JJA in the past have been done in samples with a diagonal bias. For example, van Wees, van der Zant, and Mooij[25] have observed the existence of a transverse voltage in their measurements, which was unexplained. From our finding that the [11] direction is unstable against changes in the angle of the bias, we conclude that any small deviation in the direction of the flow of current, either due to tiny fabrication defects in the busbars or to disorder in the critical currents of the junctions,[24] may explain their observation. Also Chen, Delsing, Haviland, and Claeson[26] have reported a transverse angle in measurements in JJA driven in the diagonal direction. In their case the effect is antisymmetric against a change in the direction of the magnetic field. Since transverse voltages due to the instability of the [11] direction are even with the direction of the magnetic field, their observation cannot be explained from our results. This means that they have a Hall effect, possibly due to quantum fluctuations. However, they report that their transverse voltage also had a component that was even with the magnetic field (which was discounted in their computation of the Hall angle). This particular spurious contribution can also be attributed to a small deviation in the direction of the bias or to disorder effects. From this we conclude that in order to study the Hall effect in JJA the most convenient choice would be a current bias in the [10] direction where the effect of transverse voltages at small deviations in the bias or disorder is minimum.

When this work was completed, new studies on the effect of the orientation of the bias in driven square JJA have appeared. Fisher, Stroud, and Janin[27] have studied some of the effects of the direction of current in a fully frustrated JJA ($f=1/2$) at $T=0$. In their case a transverse critical critical current and the dynamics as a function of I_x and I_y has been described. Their results are in part complementary to our work with a single vortex ($f=1/L^2$). Yoon, Choi and Kim[28] find differences in the I–V characteristics of JJA at $f=0$ when comparing the parallel current bias with the diagonal current bias. Their results are in agreement with our Fig. 3 results.

In this paper we have considered the dynamics of a single vortex in a square JJA. We were able to characterize in detail the orientational pinning and breaking of rotational symmetry in this case. Furthermore, with the results of the RSJ numerical calculation we were able to reproduce and interpret most of our experimental measurements for a quasidiagonal bias. It remains for the future to study the behavior of a driven VL when the current is rotated, since the VL also has its own periodicity and symmetry directions. As we saw recently in Ref. 12, a moving vortex lattice in a JJA shows different dynamical phases as a function of temperature and current. Therefore we expect that the characteristics of the breaking of rotational invariance, orientational pinning, and transverse voltages will depend on the dynamical phase under consideration as well as on the disorder in the Josephson couplings.[24]

ACKNOWLEDGMENTS

We acknowledge financial support from CONICET, CNEA, ANPCyT, Secyt-Cuyo, and Fundación Antorchas. One of us (P.M.) thanks the Swiss National Science Fundation for support.

*Permanent address: Departamento de Física, Universidad Nacional de Buenos Aires, Buenos Aires, Argentina.

[1] O. Daldini, P. Martinoli, J.L. Olsen, and G. Berner, Phys. Rev. Lett. **32**, 218 (1974); P. Martinoli, O. Daldini, C. Leemann, and B. Van den Brandt, *ibid.* **36**, 382 (1976); P. Martinoli, Phys. Rev. B **17**, 1175 (1978).

[2] B. Pannetier, J. Chaussy, R. Rammal, and J.C. Villegier, Phys. Rev. Lett. **53**, 1845 (1984).

[3] See for example M.S. Rzchowski, S.P. Benz, M. Tinkham, and C.J. Lobb, Phys. Rev. B **42**, 2041 (1990); For a review see: *Macroscopic Quantum Phenomena and Coherence in Superconducting Networks*, edited by C. Giovanella and M. Tinkham (World Scientific, Singapore, 1995). Proceedings of the ICTP Workshop on Josephson-Junction Arrays, edited by H.A. Cerdeira and S.R. Shenoy [Physica B **222**, 253–406 (1996)].

[4] C.J. Lobb, D.W. Abraham, and M. Tinkham, Phys. Rev. B **27**, 150 (1983).

[5] J.I. Martín, M. Vélez, J. Nogués, and Ivan K. Schuller, Phys. Rev. Lett. **79**, 1929 (1997).

[6] V.V. Moshchalkov, M. Baert, V.V. Metlushko, E. Rosseel, M.J. van Bael, K. Temst, Y Bruynseraede, and R. Jonckheere, Phys. Rev. B **57**, 3615 (1998).

[7] Y. Fasano, J.A. Herbsommer, F. de la Cruz, F. Pardo, P.L. Gammel, E. Bucher, and D.J. Bishop, Phys. Rev. B **60**, R15047 (1999).

[8] M. Franz and S. Teitel, Phys. Rev. Lett. **73**, 480 (1994); Phys. Rev. B **51**, 6551 (1995); S. Hattel and J.M. Wheatley, *ibid.* **51**, 11951 (1995).

[9] C. Reichhardt, C.J. Olson, and F. Nori, Phys. Rev. B **54**, 16108 (1996); **57**, 7937 (1998).

[10] C. Reichhardt, C.J. Olson, and F. Nori, Phys. Rev. Lett. **78**, 2648 (1997); Phys. Rev. B **58**, 6534 (1998).

[11] C. Reichhardt and F. Nori, Phys. Rev. Lett. **82**, 414 (1999).

[12] V.I. Marconi and D. Domínguez, Phys. Rev. Lett. **82**, 4922 (1999).

[13] C. Reichhardt, G. Zimanyi, cond-mat/9911044 (unpublished).

[14] T.C. Halsey, Phys. Rev. B **31**, 5728 (1985).

[15] L.L. Sohn, M.S. Rzchowski, J.U. Free, S.P. Benz, M. Tinkham, and C.J. Lobb, Phys. Rev. B **44**, 925 (1991); L.L. Sohn, M.S. Rzchowski, J.U. Free, M. Tinkham, and C.J. Lobb, *ibid.* **45**, 3003 (1992).

[16] T. Giamarchi and P. Le Doussal, Phys. Rev. Lett. **76**, 3408 (1996); P. Le Doussal and T. Giamarchi, Phys. Rev. B **57**, 11356 (1998); L. Balents, M.C. Marchetti and L. Radzihovsky, *ibid.* **57**, 7705 (1998).

[17] H. Pastoriza, S. Candia, and G. Nieva, Phys. Rev. Lett. **83**, 1026 (1999).

[18] J.J. Vicente Alvarez, D. Domínguez, and C.A. Balseiro, Phys. Rev. Lett. **79**, 1373 (1997).

[19] J.S. Chung, K.H. Lee, and D. Stroud, Phys. Rev. B **40**, 6570 (1989); F. Falo, A.R. Bishop, and S.P. Lomdahl, *ibid.* **41**, 10983 (1990); N. Grønbech-Jensen, A.R. Bishop, F. Falo, and S.P. Lomdahl, *ibid.* **46**, 11149 (1992), P.H.E. Tiesinga, T.J. Hagenaars, J.E. van Himbergen, and Joge V. José, Phys. Rev. Lett. **78**, 519 (1997).

[20] W. Yu, K.H. Lee, and D. Stroud, Phys. Rev. B **47**, 5906 (1993).

[21] T.J. Hagenaars, P.H.E. Tiesinga, J.E. van Himbergen, and J.V. José, Phys. Rev. B **50**, 1143 (1994).

[22] D. Domínguez, J.V. José, A. Karma, and C. Wiecko, Phys. Rev. Lett. **67**, 2367 (1991); D. Domínguez, *ibid.* **72**, 3096 (1994).

[23] D. Domínguez, Phys. Rev. Lett. **82**, 181 (1999).

[24] V. I. Marconi and D. Domínguez (unpublished).

[25] B.J. van Wees, H.S.J. van der Zant, and J.E. Mooij, Phys. Rev. B **35**, 7291 (1987).

[26] C. D. Chen, P. Delsing, D. B. Haviland, and T. D. Claeson, in *Macroscopic Quantum Phenomena and Coherence in Superconducting Networks*, edited by C. Giovanella and M. Tinkham (World Scientific, Singapore, 1995), p. 121.

[27] K.D. Fisher, D. Stroud, and L. Janin, cond-mat/9906068 (unpublished).

[28] M. Yoon, M.Y. Choi, and B.J. Kim, Phys. Rev. B **61**, 3263 (2000).